DEPOSITION OF MAGNETITE PARTICLES ONTO ALLOY-800 STEAM GENERATOR TUBES

M. Basset, N. Arbeau, J. McInerney and D.H. Lister

Department of Chemical Engineering, University of New Brunswick, P. O. Box 4400,
Fredericton, New Brunswick, Canada, E3B 5A3

ABSTRACT

Fouling is a particularly serious problem in the power generating industry. Deposits modify the thermalhydraulic characteristics of heat transfer surfaces by changing the resistance to heat transfer and the resistance to fluid flow, and, if thick enough, can harbour aggressive chemicals. Deposits are also implicated in the increase of radiation fields around working areas in the primary heat transfer systems of nuclear power plants.

In order to understand the preliminary steps of the formation of corrosion product deposits on the outsides of steam generator tubes, a laboratory program has investigated the deposition of magnetite particles from suspension in water onto Alloy-800 surfaces under various conditions of flow, chemistry and boiling heat transfer.

A recirculating loop made of stainless steel operating at less than 400kPa pressure, with a nominal coolant temperature of 90°C, was equipped with a vertical glass column which housed a 2.5E-01m-long Alloy-800 boiler tube capable of generating a heat flux of 240kW/m^2. A concentration of suspended magnetite of 5.0E-03kg/m^3 was maintained in the recirculating coolant, which was maintained at a pH of 7.5. The magnetite was synthesized with a sol-gel process, which was developed to produce reproducibly monodispersed, colloidal ($<1\mu$m) and nearly spherical particles. A radiotracing method was used to characterize the deposit evolution with time and to quantify the removal of magnetite particles.

The results from a series of deposition experiments are presented here. The deposition process is described in terms of a two-step mechanism: the transport step, involving the transport from the bulk of the liquid to the vicinity of the surface, followed by the attachment step, involving the attachment of the particle onto the surface. Under non-boiling heat transfer conditions, diffusion seems to be the dominant factor ruling deposition with a small contribution from thermophoresis; removal was considered negligible in this regime. Transport models based on diffusion mechanisms, however, only predict the results within a factor of about 5. Under conditions of sub-cooled boiling at a low rate, the trapping of particles by the bubble surface is an important mechanism leading to deposition; at a high bubble nucleation rate, microlayer evaporation seems to dominate.

DEPOSITION OF MAGNETITE PARTICLES ONTO ALLOY-800 STEAM GENERATOR TUBES

M. Basset, N. Arbeau, J. McInerney and D.H. Lister

INTRODUCTION

Fouling, defined as the accumulation of undesired solid material at phase interfaces, is a particularly serious problem in the power generating industry. The formation of deposits on heat transfer surfaces affects their thermalhydraulic performance by increasing the resistance to fluid flow and by changing the resistance to heat transfer. Furthermore, if thick enough, deposits can provide an environment for corrosion by harbouring aggressive chemicals [1].

Magnetite is one of the principal corrosion products formed on the carbon steel surfaces of piping and equipment of the secondary coolant system of nuclear reactors. Magnetite is released from these surfaces to the high temperature water; it is then transported by the steam generator feed water as a suspension of colloids or particle agglomerates (in the size range from below 1 to about 50μm) to the steam generator tubes, where it deposits again.

Various studies on the particular mechanisms of particle deposition onto heat transfer surfaces have been performed in the past. It is fairly well established that, under isothermal conditions, particulate deposition onto a surface is a two-step process, occurring in series: a transport step, involving the transport from the bulk of the liquid to the vicinity of the surface, is followed by an attachment step, involving the attachment of the particle onto the surface. Assuming a linear dependence with the concentration in the bulk C_b, the initial deposition particle flux ϕ_d is generally expressed mathematically by [2]:

$$\phi_d = C_b \,.\, K_d \qquad (1)$$

with $$1/K_d = 1/K_t + 1/K_a \qquad (2)$$

where K_d, K_t and K_a are respectively the deposition, transport and attachment coefficients. The transport of particles to the vicinity of the collector surface is the best understood of the fouling stages and mathematical models are available to quantify K_t. As far as the attachment step is concerned, the sticking probability approach (probability that a particle that reaches the wall will stick to it) [2] has been replaced by a more fundamental approach taking into account the surface force field between the depositing particles and the collector surface. Electrical double-layer and London-Van-der-Waals contributions will control the particle motion at small distances from the wall (1E-09 to 10E-09m) [3]. The London-Van-der-Waals contribution is usually attractive, whereas the electrical double layer contribution will strongly depend on the pH of the solution, which will influence the overall net charge on both the colloidal particles and the collector surface. Generally, if the charges exhibit the same sign, the net surface force field will be repulsive and the deposition rate will be attachment rate controlled ($1/K_d \approx 1/K_a$). If the charges on the wall and the particles are opposite, the net surface force field will be attractive, and the deposition rate will be mass transfer controlled ($1/K_d \approx 1/K_t$). In their investigation on the deposition of magnetite particles onto Alloy-800 surfaces under isothermal conditions, Turner, Lister and Smith [4] showed that the deposition rate is maximum at pH = 7.5, that deposition is limited by particle transport for pH values between 6.5 and 8.3, and that deposition is limited by the rate of attachment for pH outside this range.

In the presence of heat transfer, a thermal force is created: cold walls will enhance deposition, whereas hot walls will impede deposition. Thermophoresis has been shown to play a non-negligible role under non-boiling heat transfer conditions, at least for colloidal particles [2].

The presence of boiling heat transfer on the surface will have a great impact on the deposition of magnetite particles. Maximal deposition rates have been obtained under conditions of surface boiling, and, to a lesser extent, at the start of nucleate boiling of the flowing fluid; furthermore, the deposits formed under such conditions were relatively porous and presented relatively good heat transfer properties [5]. Turner and Godin [6] compared the magnetite deposition onto Alloy-600 steam generator tubes from pressurized non-boiling water with that from pressurized boiling water. They concluded that, when the attachment step is not limiting (unlike charges on the surface and the particles), the boiling contribution to deposition adds directly to the particle transport rate from turbulent deposition, whereas in the case where the attachment step is limiting (like charges on the surface and the particles), the contribution of boiling adds to the single phase forced convective rate taking into account both the transport and attachment step.

Thomas and Grigull [7] pointed out the importance of the "boiling factor". They performed a series of experiments on the deposition of magnetite in single- and two-phase flow. They suggested that, in two-phase flow involving heat transfer, the rate of deposition is controlled by the mode of boiling heat transfer. In the case of nucleate boiling, the rate of deposition increased linearly with the heat flux. The authors suggested a possible correlation between the deposition rate increase and the number of bubbles formed per unit surface area and time. According to them, the formation of bubbles produces an increase in the turbulence in the boundary layer adjacent to the wall, combined with an increasing flow of water and magnetite in the direction of the wall to replace the space occupied by the leaving bubbles. In the case of film-boiling heat transfer, a continuous blanket of vapor is formed on the surface, thus preventing any formation of deposit.

Asakura [8] studied the deposition of an α-Fe_2O_3 suspension (average particle size 3.5µm) onto Zircaloy-2 tubes in demineralized boiling water at atmospheric pressure. He observed ring-like iron oxide deposits, mainly at the sites of continuous bubbling on the heated surface. He proposed a model based on the assumption that the deposit is formed by microlayer evaporation. The microlayer is a thin layer of liquid formed underneath a growing bubble. Heat is primarily transferred from the heated surface to the surrounding liquid through the evaporation of this microlayer. The shape and formation mechanisms of the microlayer have been studied by various authors [9] [10]. Asakura suggested that the particles in suspension deposit at the same time as a dry patch in the centre of the microlayer grows.

According to Asakura's model, a deposit is expected to show concentric rings, and is supposed to be thicker at its extremity because the volume of liquid that evaporates during bubble growth is higher on the periphery than in the centre of the microlayer. Thorne and co-workers [11], in their study of magnetite particle deposition under sub-cooled conditions onto Alloy-800 surfaces, have demonstrated the formation of such deposits. They clearly showed as well an increase in the initial deposition rate with the heat flux.

This study investigates further the mechanisms and kinetics of deposition under boiling and non-boiling heat transfer in the sub-cooled mode. For that purpose, a laboratory program has investigated the deposition of magnetite colloidal particles from suspension in water onto Alloy-800 surfaces, under both surface-boiling and non-surface-boiling conditions. An on-line radiotracing technique was used to follow the long term deposition and removal behavior of particles.

EXPERIMENTAL

Magnetite Synthesis

The magnetite particles used in the experiments have been synthesized using a sol-gel method described by Sugimoto and Matijevic [12]. The formation of magnetite particles is the result of the aging at 90°C and in an oxygen-free environment of a ferrous hydroxide gel formed by interaction of ferrous sulfate with potassium hydroxide in the presence of nitrate ions. The magnetite particles prepared in this way were characterized by SEM to determine their size and morphology and by X-ray analysis to confirm the formation of magnetite crystals. The point of zero charge of the particles (PZC - pH at which the particles have no net charge) was also measured.

Low Temperature Recirculating Loop

A recirculating loop made of stainless steel was set up as shown in figure 1. The vertical test section is comprised of a 1.5m glass column having an inner diameter of 9.93E-02m. The column houses a 30.0E-02m-long and 1.59E-02m-diameter Alloy-800 boiler tube equipped with a 25.0E-02m-long cartridge heater capable of generating a maximum heat flux of 240kW/m^2. The heating element is packed in the boiler tube with aluminum powder to provide an evenly-distributed heat flux. The leading end of the tube (made of stainless steel 304) has been machined in order to ensure a smooth and even upward flow around the boiler tube. The glass column and the piping are insulated in order to prevent any heat loss. Two 170L tanks equipped with Caloritec heaters connected to a control board are able to maintain a magnetite suspension in the coolant at a constant temperature up to 95°C. The tanks are equipped with nitrogen gas purging systems to maintain a relatively inert atmosphere in the system. While one tank is normally valved in during an experiment, when radioactive tracing is in progress the two tanks, one with non radioactive suspension and the other one with radioactive material, can be valved in in turn. A by-pass line is used to divert the flow in case the tube has to be removed from the test section for analysis. The flow is provided by a stainless steel centrifugal pump capable of delivering a range of flows up to a Reynolds number of 7250 as measured in the test section. A second pump was eventually installed in the circuit, so that the two pumps in series covered a range of flow rates up to a Reynolds number of 15133 and slightly pressurized the system at the same time. Pressures up to 360kPa in the test section can now be reached. A pressure gauge is used to measure the pressure in the loop and to detect any drop in the flow rate (the pressure is a known function of the flow rate in the test section).

Experiments

Three runs were performed (see table 1). In each run, the loop was filled with approximately 80L of de-ionized water preheated to 90°C. The water was purged constantly with nitrogen for at least 24 hours before starting an experiment. Temperatures at the outlet of the test section were always maintained below 100°C during the experiments, so that massive bulk boiling was avoided. A solution of suspended magnetite at the same pH as the water loop was used to fix the concentration of magnetite at the required level. In order to compensate for the loss of magnetite in the system (sedimentation in the tank, deposition of magnetite on the stainless steel tubing and on various pieces of equipment of the loop), a reservoir of magnetite in suspension (1.0E-01 kg/m^3) was constantly supplying the main loop at a regulated rate. The magnetite concentration was regularly checked by atomic absorption spectrometry of withdrawn samples and was subsequently adjusted. The pH of the system was regularly checked also and fixed at a pH value of 7.5 by addition of 0.1, 0.01 or 0.001M nitric acid or potassium hydroxide solutions. At the start of a run, the Alloy-800 tube was carefully cleaned with acetone and a dilute nitric acid solution and generously rinsed with de-ionized water before its immersion in the test section. The pattern of deposition was studied with an optical microscope.

i) In run #1, deposition of magnetite particles under sub-cooled boiling conditions was studied by a gravimetric method. After a given period of time, the Alloy-800 boiler tube was carefully taken out of the test section and the magnetite was removed from the tube and dissolved in a 10^{-3}M HCl solution stirred for 30 minutes at 90°C. The iron content of the digested sample was analyzed with the Perkin Elmer 3100 atomic absorption spectrometer (wavelength: 302.1nm; glass bead injector). The experiment was repeated for different durations up to 50 hours. The thermodynamic quality of the two-phase system is unknown.

ii) In run #2, deposition of magnetite particles under non-boiling conditions was studied using a gravimetric technique. The second pump in the circuit was used to pressurize the test section slightly, so that surface boiling did not occur. It was then possible to compare the deposition of magnetite in the absence of boiling, under the same conditions of heat flux, pH, chemistry and flow rate, with that in the presence of boiling in run #1. The experiment was repeated for different durations up to 50 hours.

iii) In run #3, deposition of magnetite particles under sub-cooled boiling heat transfer was determined as a function of time by a radiotracing technique. Two 3g samples of magnetite were irradiated for 15 hours in the McMaster Research reactor to produce Iron-59, a gamma emitter (half life = 45 days). Each sample of magnetite was mixed with 3.5g of non-radioactive magnetite and added to the tank to maintain the concentration at about 5.0E-03kg/m^3. The activity of Fe-59 was determined on-line by measuring the intensity of the gamma ray at 1095keV with a germanium gamma-detector positioned in front of the tube. The magnetite source was switched in the middle of the experiment to a non-radioactive magnetite by valving in the second tank; this was in order to quantify any mechanism involving a release of material from the surface. The source was then switched back to the radioactive material at a different concentration (11.2E-03kg/m^3). The specific activity of the magnetite in suspension was continuously monitored by sampling the circulating water. The thermodynamic quality of the two-phase system is unknown.

RESULTS

Magnetite Synthesis

The X-ray analysis confirmed the formation of magnetite particles. A SEM picture of the magnetite prepared for that study is shown in figure 2. The particles are monodispersed and their shape is nearly spherical with an average diameter of 0.6μm. The excellent quality of the synthesis product is a result of a contact recrystallisation mechanism [12]. The point of zero charge of the magnetite prepared for this study was 5.9 and the zeta-potential at pH = 7.5 was about -17.0E-03V under the following conditions: magnetite suspension concentration about 20E-03kg/m^3; potassium nitrate concentration about 0.001M. The PZC of magnetite is usually about 6.4 at room temperature [4], but values have been shown to depend strongly on the temperature, the way the magnetite is synthesized, and the conditions under which the measurements are taken. In particular, the PZC will vary with the particle concentration, the ionic strength of the medium and the concentration of the counterions [13].

Magnetite Deposition

i) The results of runs #1 and #2 are presented in figure 9. Under non-boiling conditions (run #2), the deposition seems to be a linear function of time. Microscope examination indicated that, on the Alloy-800 surface, the deposit is uniform around the tube, but varies in the vertical direction, i.e. with the flow. A relatively heavy deposit is present at the bottom of the tube, but this diminishes towards the top of the column, so that at a distance of about 2.0E-01m from the "nose" of the tube there is hardly any deposit. The overall fouling rate seems to be linear for the first 50 hours (figure 9). The measurements therefore indicate a constant deposition velocity (deposition rate divided by source term or concentration), which amounts to 3.2E-07m/s. The deposition pattern may be described using a diffusion mechanism including thermophoresis effects.

Under sub-cooled boiling conditions, the deposition rate falls off with time. The deposition patterns presented in figures 3, 5 and 6 suggested important differences in the mechanisms involved under boiling and non-boiling conditions. Consider, for example, a boiling experiment. The tube is positioned vertically in the test section. As the fluid flows along the tube, the surface temperature and the fluid temperature at the interface will vary. The tube will have two regions with specific heat transfer characteristics - non-boiling and sub-cooled boiling:

- near the "nose" of the tube, the fluid temperature at the interface is still close to the inlet temperature (90°C), and the temperature conditions on the tube and in the fluid at the interface do not allow bubble nucleation. The conditions of heat transfer are similar to those in run #2, and a relatively heavy deposit that resembles the one observed in run #2 can be observed (compare figures 3 and 5).

- as the fluid flows along the tube, its temperature in the vicinity of the surface increases, and the thermal boundary layer thickens. The surface temperature increases slightly as well. Therefore, further along the tube, bubbles can nucleate on the surface. Cooper and Lloyd [9] clearly demonstrated that bubble growth rate depends on the balance between the rate of microlayer evaporation and the rate of condensation over the surface of the bubbles. The bubble characteristics (size, shape, growth rate) will change along the tube as the temperature on the tube and the fluid temperature at the interface vary.

In the lower part of the tube, because of the relatively cool temperature of the fluid at the interface, bubbles will grow very slowly on the surface (growth periods were observed to extend to a minute) and will mostly collapse while still attached to the surface. The boiling activity is limited, and the maximum bubble diameter is relatively large (1E-03 to 2E-03m). The deposit characteristics change completely with the appearance of bubbles, suggesting a completely different deposition mechanism from that in non-boiling (see figure 5). Ring-shaped deposits about 1.0E-04 to 2.0E-04m across are formed. We observed that magnetite particles collect on the bubble surface (see figure 8). As the bubble grows, particles are continually swept down to the tube surface where they deposit, thus explaining the ring pattern of these deposits (see figure 7a). As bubbles collapse, they release particles that were trapped in the vapour-liquid interface, thereby ensuring a relatively high magnetite concentration near the tube surface. After a long period, the deposit becomes relatively heavy by accumulating slowly around the bubble nucleation point, and nucleation is stifled.

Further along the tube, the temperature of the fluid at the interface is higher and bubbles can depart from the surface, but will rapidly collapse in the vicinity of the surface because of the sub-cooled conditions. At a given nucleation site, bubbles are nucleating at a much faster rate (1 to 3 bubbles per second on average) and leaving the surface; the maximum bubble diameter is smaller than in the lower part of the tube. Now, circular spots or discs of black deposit are mainly formed (figure 4). These spots are smaller than the ones observed in the lower part of the Alloy-800 surface. The spot pattern is fairly well described by a mechanism based on the evaporation of a microlayer underneath the growing bubble as suggested by Asakura [8]. The shape and size evolution of the microlayer is given in figure 7b. Microlayers are wedge-shaped in cross section - their thickness increases from the centre of the bubble to its extremity. The thickness of the microlayer changes during bubble growth. Near the microlayer centre its thickness diminishes progressively with time, whereas at the outer edge its thickness increases with time, suggesting the existence of a fluid current replenishing the microlayer at a rate exceeding the rate of liquid evaporation [10]. The particles in suspension deposit at the same time as a dry patch in the centre of the microlayer grows (figure7b).

ii) The results of run #3 are presented in figure 10. Data are corrected for decay to valve-in time. The intensity of the gamma ray at 1095keV was recorded every half an hour. For clarity reasons, the graph only shows the data points every two hours. The radiation background was evaluated prior to the insertion of the tube in the loop and after its withdrawal at the end of the run, in order to determine the evolution of the background during the experiment. We assumed that the background followed the same trend as the overall build-up given by the experimental data points. The build-up on the tube was then obtained by subtracting the background data from the experimental data. Figure 10 presents the build-up of radioactivity on the tube as a function of time obtained by this method.

The evolution of the source term (activity per unit volume of magnetite in suspension) was monitored as well during the experiment. Using this value as the driving force for the deposition process, the Kern and Seaton model for the corresponding activity build-up on the Alloy-800 tube was evaluated and compared with the experimental data (see discussion and figure 10). The good correspondence between the data and the theory is in favour of a concomitant release and deposition model. In particular, the rather slow readjustment of the source term after the flow switch at 390 hours is accommodated very well by the model.

DISCUSSION

Deposition Under Non-Boiling Heat Transfer (Run #2)

The overall fouling rate seems to be linear for the 50 hours of the experiment (figure 9) and amounts 3.2E-07 m/s. The fouling process is considered to be the combination of two competitive stages, which usually occur simultaneously: the formation of the deposit and the removal of the deposit.

$$\frac{dm_f}{dt} = K_d.C_b - k_r.m_f \qquad (3)$$

where m_f is the mass of fouling material on the surface, and k_r a coefficient characterizing the removal rate. When boiling is absent, other authors also have reported that removal is insignificant in the case of colloidal particles [2]. Consequently, we have a linear behavior, $k_r = 0$ and $C_b = 5E\text{-}03\ kg/m^3$; therefore equation (3) will give $K_d = 3.2E\text{-}07$ m/s.

The deposition behavior may be explained using a diffusion mechanism including thermophoresis. Thus, we postulate a two-step mechanism: a transport step, involving the transport from the bulk of the liquid to the vicinity of the surface, followed by the attachment step, involving the attachment of the particle onto the surface. At a pH value of 7.5, the net surface charge of the synthesized magnetite (PZC at room temperature: 5.9) is negative and the net charge on the Alloy-800 surface (PZC at room temperature: 8.0 [4]) is positive. Therefore, the surface force field at the interface is attractive, and the deposition rate is limited by the particle transport rate. Under these conditions, the deposition coefficient K_d is equivalent to the transport coefficient K_t.

For the transport of particles to a surface under isothermal turbulent flow conditions, the rate of mass transfer is a function of the dimensionless particle relaxation time t_p^+ [14]. In a liquid, the rate of mass transfer under turbulent flow conditions is dominated by diffusion if t_p^+ is less than 0.01; inertial effects contribute significantly if t_p^+ is more than 0.02 and dominate if t_p^+ is more than 0.2. The magnitude of t_p^+ in our study is of the order of 1.6E-05, hence diffusion should be the dominant transport mechanism. Metzner and Friend [15] described this situation, giving the following semi-empirical relation for the rate constant for particle transport, assuming that the diffusion coefficient of the particles can be equated to the Brownian diffusion coefficient.

$$K_d = K_t = 0.084u^*/\ Sc^{0.67} \qquad (4)$$

where the friction velocity u^* is a function of the shear stress at the wall and of the average velocity in the annulus, and Sc is the Schmidt number. Under the present conditions, the friction velocity u^* = 2.0E-02 m/s, the Schmidt number Sc = 1.2E+05, and therefore the theoretical particle transport to the wall is K_t = 6.7E-08 m/s - considerably less than the experimental K_d obtained from equation (3).

Thermophoresis effects may contribute to the varying deposition along the tube. Thus, as the fluid flows along the tube, its temperature in the vicinity of the surface increases, and the thermal boundary layer thickens. The surface temperature of the tube will increase slightly as well. This will result in an increasing thermophoretic barrier in the vertical direction of the flow. If we include thermophoresis acting in conjunction with diffusion, the resulting overall flow rate of particles towards the heated surface ϕ_d becomes [2]:

$$\phi_d = \left(\frac{0.084u^*}{Sc^{2/3}} - 0.26\,\frac{1}{2\lambda_l + \lambda_p} \times \frac{\nu_f}{2T} \times Q\right)C_b \qquad (5)$$

where λ_l and λ_p are respectively the thermal conductivity of the liquid and the particles, T is the temperature of the fluid, ν_f the fluid kinematic viscosity, and Q the heat flux. The thermal conductivity of magnetite is λ_p = 1.7W/(m.K) [5] and C_b=5E-03kg/m^3. Therefore, the predicted deposition rate according to equation (5) is K_t = 6.4E-08m/s; this is only slightly less than the value calculated with equation (4), indicating that thermophoresis should have only a small effect.

The theory clearly gives only a rough idea of the deposition rate; experimental values reported in the literature do not match very well the predicted values either. Turner [14] in a comprehensive analysis of particulate deposition, pointed out the large scatter of experimental values around the predicted values. Several explanations can be put forward for these differences. For example, the predicted rate has been calculated assuming that the Alloy-800 surface was smooth; surface roughness is expected to enhance deposition by reducing the thickness of the viscous sublayer.

Also, the model represented by equation (5) does not take into account hydrodynamic forces such as the drainage force and the lift force, that have been shown to influence greatly particle transport to a surface in a liquid [1]. In that case, the particle diffusion coefficient is a complicated and unknown function of the distance between the surface of the particle and the wall, the shape of the wall at the point of impact and the direction of particle motion.

The model gives only an average value of the deposition rate on the entire surface of the tube. It does not account for the non-uniform deposition pattern in the vertical direction. A more comprehensive model would take into account the development of the thermal boundary layer over the tube surface, the influence of this on thermophoresis, and the effect of a depleted source term as deposition progresses with distance.

Finally, the model is established for the transport of particles into a fully developed turbulent flow. Under the present conditions, the length of the Alloy-800 tube (3.0E-01m) is only 3.5 times the hydraulic diameter of the test section (8.34E-02m), which does not allow the establishment of the boundary layer on the tube, and might account as well for the discrepancy between the measured and predicted deposition rates.

Deposition Under Sub-Cooled Boiling Conditions (Run #1, same heat flux as Run #2; Run #3, twice heat flux of Runs #1 and #2)

Under sub-cooled boiling conditions, the deposition rate falls off with time and removal is shown to be an important factor of the fouling process since a shift to inactive material caused a decrease in surface activity, even though the mass deposited should not have changed (see figure 10). Removal has been studied before, mainly under isothermal conditions. It is generally assumed that removal is proportional to the shear stress at the wall, and its relative importance is dependent on the strength of the cohesive forces within different layers of the deposit and the adhesive forces between the particles and the collector surface. Removal is usually attributed to the unsteady character of the viscous sublayer; in particular, the vertical component and mostly the parallel component of the hydrodynamic forces acting at the wall have been shown to be responsible respectively for sudden ejection of fluid from the surface and for inducing a rolling motion to the particles prior to their final removal [16]. Under heat transfer conditions, thermal stress is believed to contribute to removal, by weakening the cohesive/adhesive forces of the deposit. However, the hydrodynamic currents associated with the departure of a bubble and the corresponding in-flow of liquid to the surface are believed to contribute to removal. Deposits around a nucleation site may reach a saturation point where deposition rate by microlayer evaporation compensates exactly the removal rate and leads to a levelling off the deposit amount.

The experimental results are compared to the Kern and Seaton model [2]:

$$\frac{dm_f}{dt} = K_d C_b - k_r m_f \qquad (3)$$

Consequently, for a clean surface at t=0:

$$m_f = \frac{K_d C_b}{k_r}(1 - \exp(-k_r.t)) \tag{6}$$

Best fit values for K_d and k_r were 3.8E-07 m/s and 3.7E-06 s^{-1} respectively for run #3, and 3.5E-07 m/s and 8.9E-06 s^{-1} respectively for run #1.

Detailed analysis of data in figure 9 shows that the initial deposition rate in sub-cooled boiling (run #1) slightly exceeds the corresponding rate in non boiling (run #2). Thomas and Grigull [7] reported that the turbulence associated with bubble departure from the surface is responsible for an influx of liquid and particles in suspension to the surface to replace the volume previously occupied by the bubble. The transport of magnetite is therefore enhanced by the bubbling. Moreover, as noted previously, under sub-cooled conditions magnetite particles are collected on the bubble surface and will be released as the bubbles collapse in the immediate vicinity of the surface, thus ensuring a relatively high concentration at the interface. However, the increase of the initial deposition rate under sub-cooled boiling conditions remains small, presumably because of the relatively small boiling activity under the present conditions.

Furthermore, in the zone where bubbles nucleate, deposit is formed exclusively at the sites of bubble nucleation (figures 4,5 and 6), suggesting that microlayer evaporation and the trapping of magnetite particles at the vapour-liquid interface are preponderant in the deposition process. Figure 5 in particular shows the sudden change in the deposition pattern after the appearance of bubbles. Beyond that point, no deposit resembling the pattern on non-boiling surfaces (postulated to be by diffusion) is observed between bubble nucleation sites (see figures 4, 5, and 6). We believe that the vapour-liquid interface is a favourable site for particle trapping due to surface tension effects, therefore excluding a relatively large area around the bubble for deposition by diffusion, which would occur normally without boiling. As already pointed out, the outer edge of the microlayer thickens with time, suggesting the existence of a fluid current replenishing the microlayer at a rate exceeding the rate of liquid evaporation. This current might also contribute to the mechanism by diverting particles to the base of the bubble where they continuously replenish the microlayer with magnetite. Furthermore, the two mechanisms described in figure 7a and 7b are believed to occur simultaneously. Their relative contributions in the overall deposition rate are suggested to depend mainly on the frequency at which bubbles are formed and depart from the surface. At the bottom of the tube, the bubble average residence time on the surface of the tube is relatively long and its radius is relatively large. Therefore, the quantity of magnetite collected at the vapour-liquid interface of a bubble is important, and the rate of deposition by the mechanism described in figure 7a will contribute mostly to deposition, whereas deposition by microlayer evaporation will be relatively low. Ring-shaped deposit will be preferentially formed. On the other hand, further along the tube, the bubble formation frequency at a given nucleation site is higher, the bubble radius is smaller and the average residence time of a bubble on the surface of the tube is shorter. Therefore, the quantity of magnetite collected on the surface of the bubble is much smaller, and the rate of deposition by microlayer evaporation is more important. Small black spots will be preferentially formed.

In boiling water, the initial deposition rate is usually considered to be proportional to the heat flux and the concentration [8]. Under sub-cooled conditions however, our initial deposition rate is increased by a factor of only 1.1 as the heat flux is almost doubled. In run #3 the data set for the whole run is adjusted to the single measurement of deposit at the end of the run and depends strongly upon the background correction, whereas in run #1, every data point is an independent measurement. The uncertainty is therefore higher in run #3 than in run #1, and no doubt contributes to the apparently small effect of doubling the heat flux. At the lower heat flux, the surface coverage by these deposits is small and increases with the heat flux. The number of active nucleation sites is known to increase with the surface temperature and the heat flux [5], and consequently more deposit rings and spots are formed per unit surface; the number of deposit rings and spots is closely related to the density of nucleation sites. In fact, a recent study in this laboratory based on a gravimetric method showed that the initial deposition rate strongly depends on the heat flux between 90 and 220kW/m^2. The detailed results of these experiments will be published in the near future.

CONCLUSIONS

- The method used to synthesize magnetite gives an excellent product of monodispersed and nearly spherical colloidal magnetite particles with a narrow size distribution.

- Under non-boiling conditions and at pH = 7.5, the rate of deposition of magnetite particles onto an Alloy-800 surface is constant and characterized by a deposition coefficient of 3.2E-07 m/s. Diffusion is believed to be the main mechanism controlling the deposition, while thermophoresis effects are calculated to play a small role. Removal is apparently negligible. Predictions based on a diffusion model are within a factor of 5 of the results.

- Under sub-cooled boiling conditions, the mechanisms of deposition are controlled by microlayer evaporation and by the processes of bubble nucleation and bubble growth. The rate of deposition falls off with time. Removal was shown to be an important part of the fouling process in this regime, and the Kern and Seaton model describes very well the experimental data.

- Deposition under sub-cooled conditions, as far as could be deduced within the scatter of results, appears to be a weak function of heat flux.

ACKNOWLEDGMENTS

This work was performed under the auspices of the Chair of Nuclear Engineering in the Chemical Engineering Department at the University of New Brunswick. The authors are grateful to the Natural Sciences and Engineering Research Council of Canada, Atomic Energy of Canada Ltd. and New Brunswick Power for financial support.

REFERENCES

[1] D. H. Lister; "Corrosion Products in Power Generating Systems", Proceedings of the International Conference on the Fouling of Heat Transfer Equipment (Rensselaer Polytechnic Institute - August 1979); from "Fouling of Heat Transfer Equipment", E. F. C. Somerscales, J. G. Knudsen, Hemisphere Publishing Corporation, pp.135-200, 1981

[2] N. Epstein; "Particulate Fouling of Heat Transfer Surfaces: Mechanisms and Models", from L. F. Melo et al. editions, "Fouling Science and Technology", pp. 143-164, Kluwer Academic Publishers, 1988.

[3] B. D. Bowen, N. Epstein; "Fine Particle Deposition in Smooth Parallel-Plate Channels", Journal of Colloid and Interface Science, Vol. 72(1), 1979.

[4] C. W. Turner, D. H. Lister, D. W. Smith; "The Deposition and Removal of Sub-Micron Particles of Magnetite at the Surface of Alloy-800", presented at the Steam Generator and Heat Exchanger Conference, Toronto, Canada, 1990.

[5] J. G. Collier; "Heat Exchanger Fouling and Corrosion", from "Heat Exchangers - Thermal-Hydraulic Fundamentals and Design", S. Kakac, A. E. Bergles, F. Mayinger, Hemisphere Publishing Corporation, p. 999-1011, 1981.

[6] C. W. Turner, M. Godin; "Mechanisms of Magnetite Deposition in Pressurized Boiling Water and Non-Boiling Water", Steam Generator and Heat Exchanger Conference, Conference Proceedings, Vol. II, Toronto 1994.

[7] D. Thomas and U. Grigull; "Experimental Investigation of the Deposition of Suspended Magnetite from the Fluid Flow in Steam Generating Boiler Tubes", Brennst-Warme-Kraft, 26(3), pp. 109-115, 1974.

[8] Y. Asakura, M. Kikuchi, S. Uchida, H. Yusa; "Deposition of Iron Oxide on Heated Surfaces in Boiling Water", Nuclear Science and Engineering, Vol. 67, pp. 1-7, 1978.

[9] M. G. Cooper, A. J. P. Lloyd; "The Microlayer in Nucleate Pool Boiling", Int. J. Heat Mass Transfer, Vol. 12, pp. 895-913, 1969.

[10] H. H. Jawurek; "Simultaneous Determination of Microlayer Geometry and Bubble Growth in Nucleate Boiling", Int. J. Heat Mass Transfer, Vol. 12, pp. 843-848, 1969.

[11] M. Thorne; Private Communication; Dept. of Chem. Eng., University of New Brunswick, 1994.

[12] T. Sugimoto, E. Matijevic; "Formation of Uniform Spherical Magnetite Particles by Crystallization from Ferrous Hydroxide Gels", Journal of Colloidal and Interface Science, Vol. 74 (1), 1980.

[13] T. M. Riddick; "Control of Colloid Stability through Zeta Potential", Livingston Publishing Company, 1968.

[14] C. W. Turner; "Rates of Particle Deposition From Aqueous Suspensions in Turbulent Flow; a Comparison of Theory with Experiment", Chemical Engineering Science, Vol. 48 (12), pp. 2189-2195, 1993.

[15] A. B. Metzner, W. L. Friend; "Theoretical Analogies between Heat, Mass and Momentum Transfer and Modifications for Fluid of High Prandtl or Schmidt Number", Canadian Journal of Chemical Engineering, Vol. 36, p. 235-240, 1958.

[16] J. Visser; "Adhesion and Removal of Particles II", from "Fouling Science and Technology", L. F. Melo et al Editions, pp. 105-123, Kluwer Academic Publishers, 1988

TABLES AND FIGURES

	Boiling Conditions (Run#1)	Non-boiling Conditions (Run#2)	Boiling Conditions Radiotracing technique (Run#3)
Heat Flux (kW/m^2)	100	100	190
Reynolds Number	7250	7250	7250
Magnetite Concentration (kg/m^3)	5.0E-03	5.0E-03	5.0E-03 for t < 390 hours 11.2E-03 for t > 390 hours
pH at 25°C	7.5	7.5	7.5
Coolant Temperature (°C)	90	90	90
Pressure (kPa)	1.6E+02	3.5E+02	1.6E+02
Deposition Constant K_d (m/s)	3.5E-07	3.2E-07	3.8E-07
Removal Constant k_r (s^{-1})	8.9E-06	0	3.7E-06

Table 1: Magnetite Deposition Experiments - Experimental Conditions and Main Results

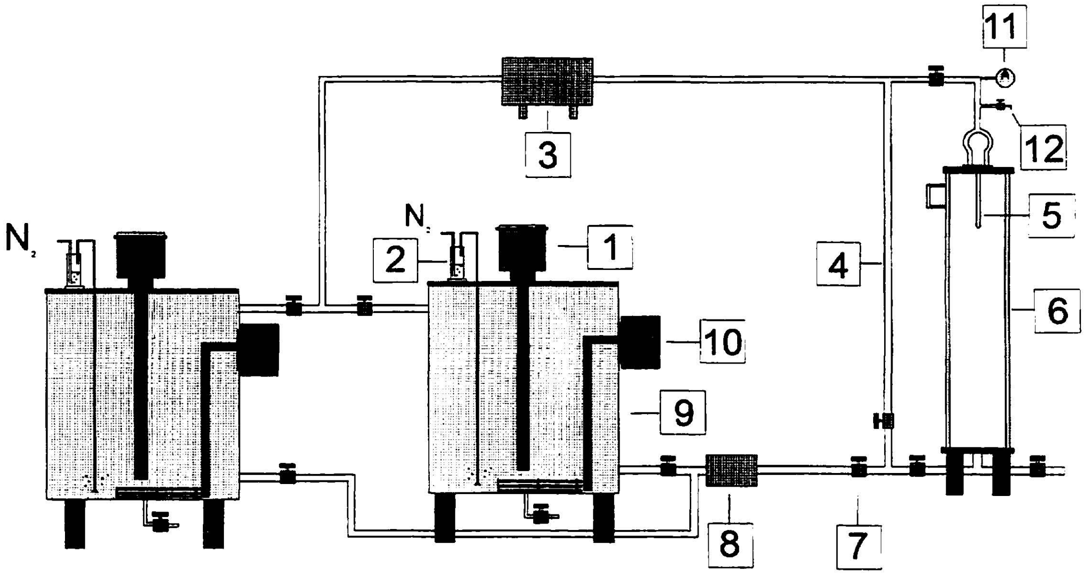

1 Stirrer	5 Alloy-800 Tube	9 Stainless Steel Reservoir
2 Nitrogen Bubbling System	6 Glass Column	10 Heater
3 Heat Exchanger	7 Valve	11 Pressure Gauge
4 By-pass Section	8 Stainless Steel Centrifugal Pump	12 Sample

Figure 1: Apparatus Set-Up

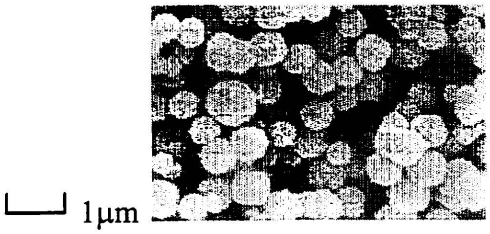

Figure 2: SEM of the Magnetite Particles Prepared by a Sol-Gel Method

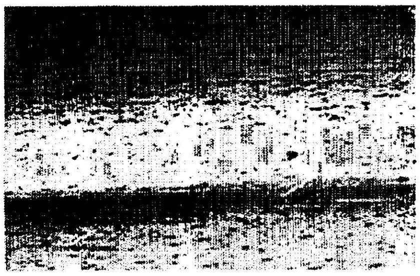

Figure 3: Deposition Under Non-Boiling Conditions After 50 Hours Run #2 - 10 cm from the "nose" of the tube

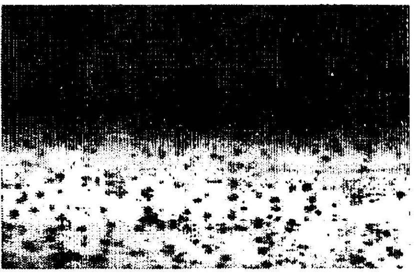

Figure 4: Deposition Under Sub-Cooled Boiling Conditions After 700 Hours Run #3- 10 cm from the "nose" of the tube

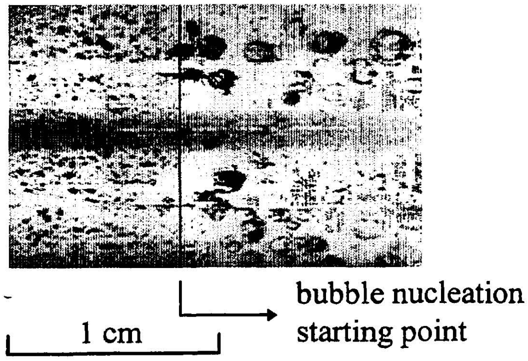

Figure 5: Deposition Under Sub-Cooled Boiling Conditions After 50 Hours Run #1 - bubble nucleation starting point

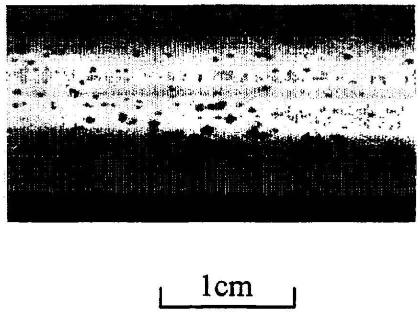

Figure 6: Deposition Under Boiling Conditions After 50 Hours Run #1 - 10 cm from the "nose" of the tube

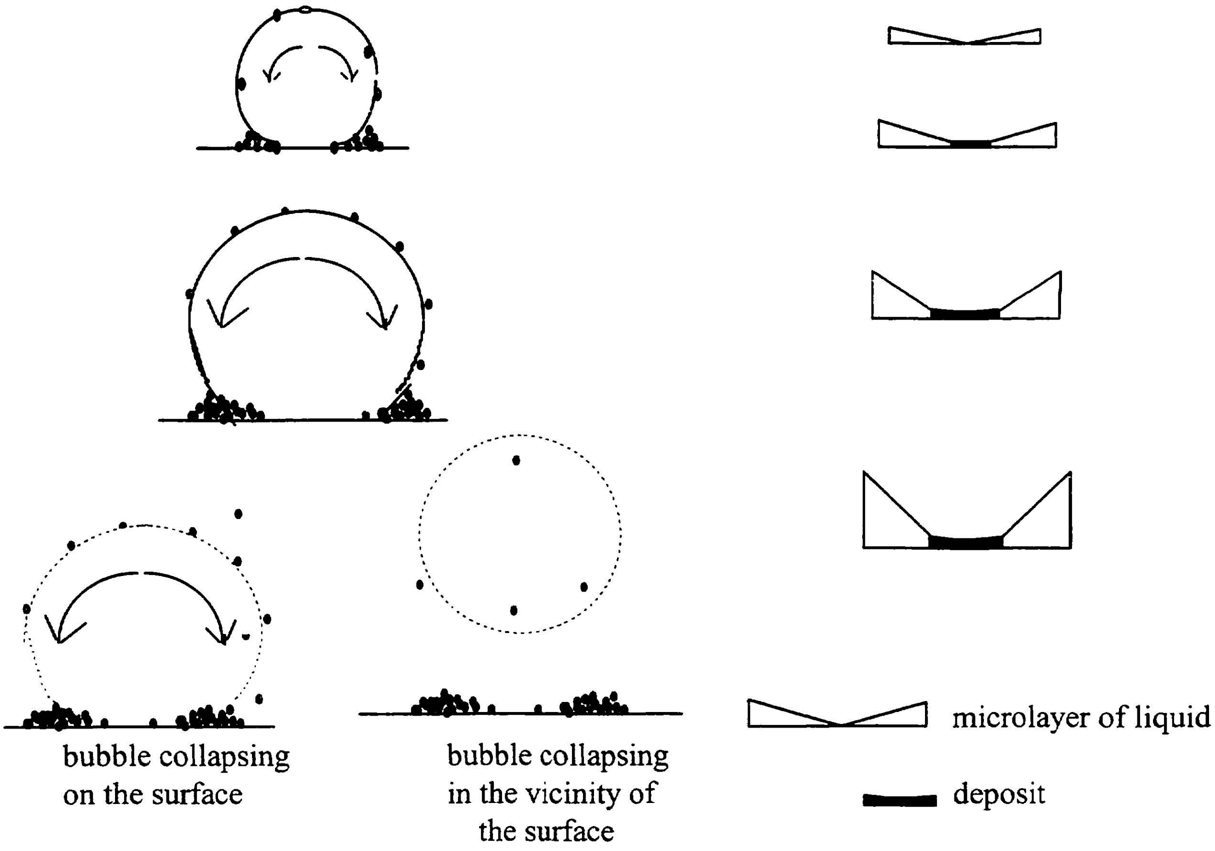

Figure 7a and 7b: Proposed Mechanism for Deposition Under Sub-Cooled Boiling Conditions
7a - Sub-Cooled Conditions
7b - Microlayer Shape and Thickness Evolution

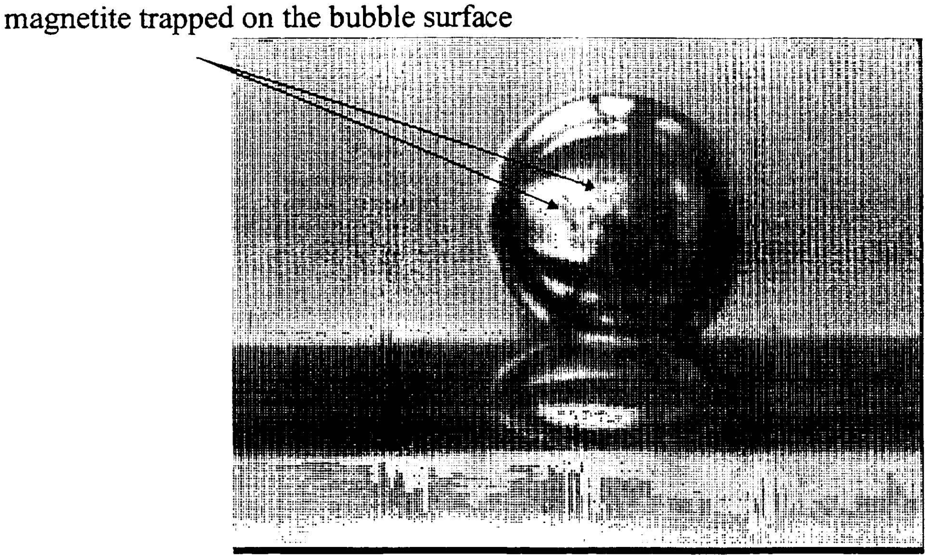

Figure 8: The Trapping of Magnetite Particles at the Liquid-Vapour Interface

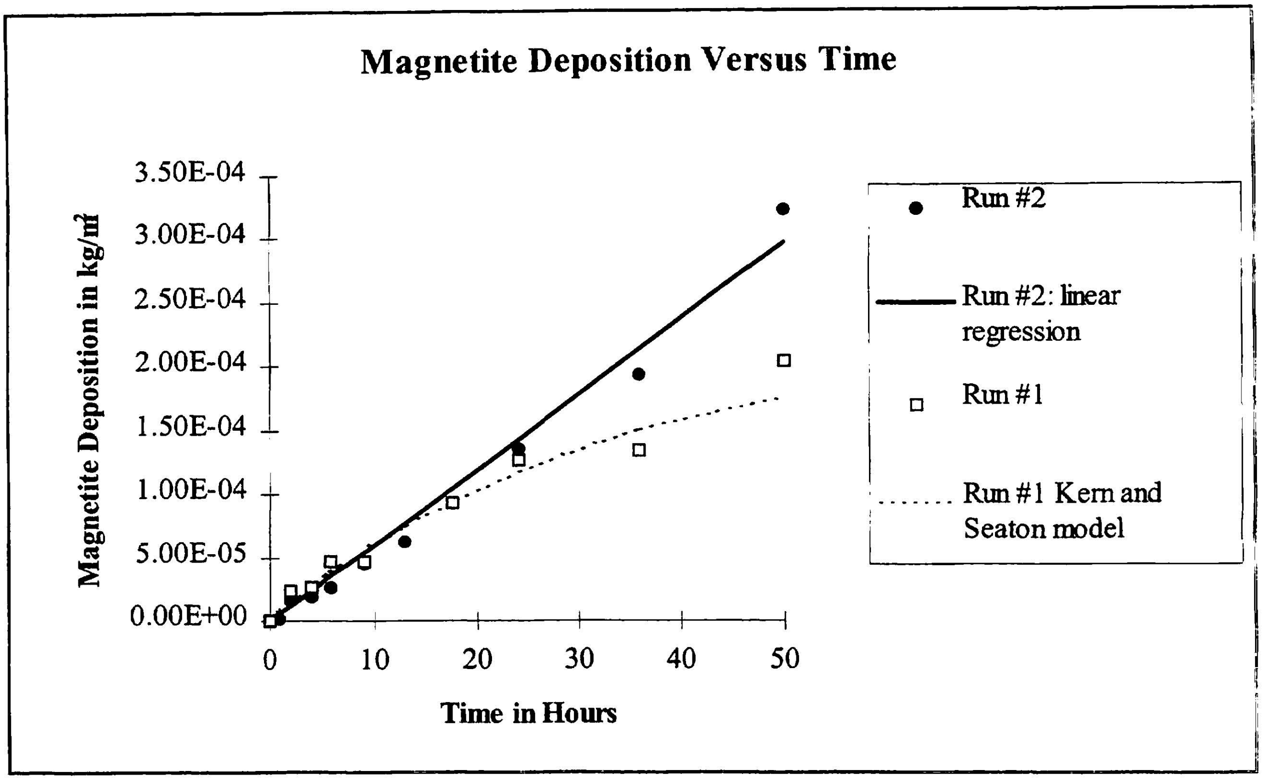

Figure 9: Deposition Versus Time (Runs # 1 and 2)

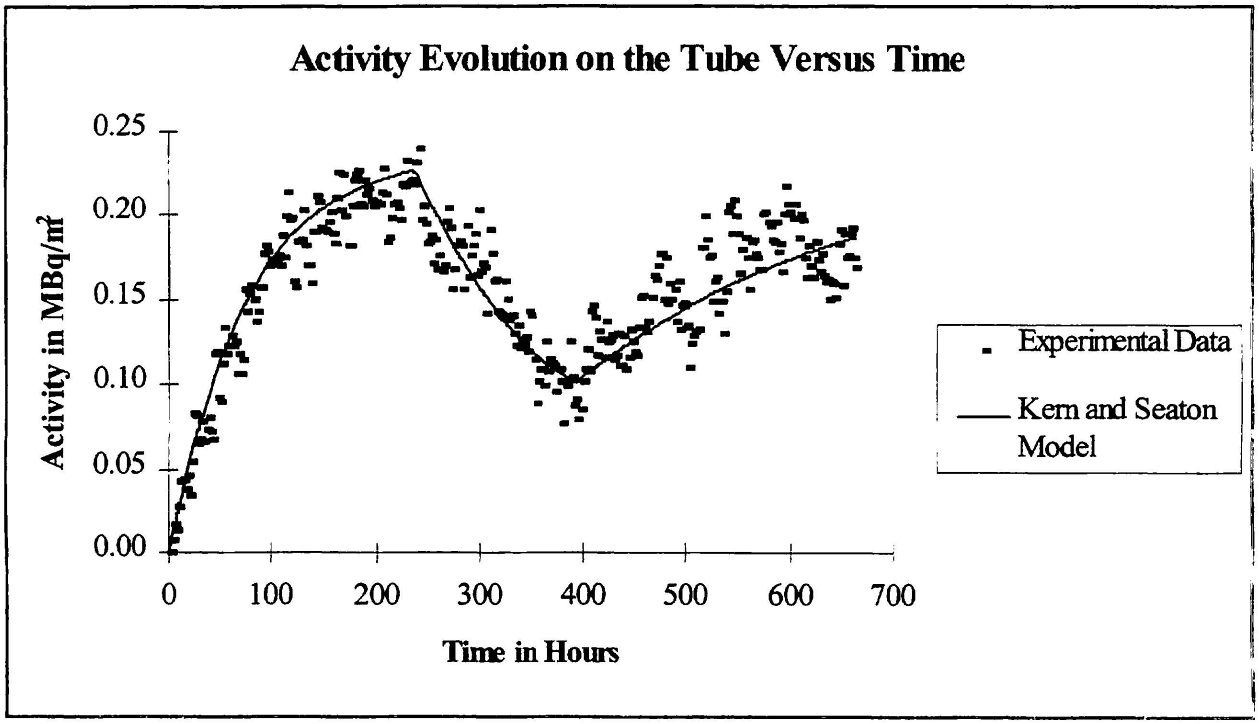

Figure 10: Deposition Versus Time (Run # 3)